QIRT 10
http://dx.doi.org/10.21611/qirt.2010.097
10th International Conference on Quantitative InfraRed Thermography
July 27-30, 2010, Québec (Canada)

Ultrasound lock-in thermography as a quantitative technique for quality control assessment of cast iron turbocharger components

by R. Montanini*, G.L. Rossi** and F. Freni*

*Department of Industrial Chemistry and Materials Engineering, University of Messina, C.da di Dio, Sant'Agata di Messina, I-98166, Italy, rmontanini@ingegneria.unime.it, ffreni@ingegneria.unime.it
**Department of Industrial Engineering, University of Perugia, Via Duranti 1, I-06125, Italy, gianluca@unipg.it

Abstract

This paper explores the application of ultrasound activated infrared thermography for the detection and quantification of flaws in industrial cast iron turbocharger components. The use of amplitude modulated ultrasonic heat generation allowed selective response of defected area, since the defect itself is turned into a local thermal wave emitter. Due to the very fast cycle time (< 30 s/part), the method could potentially be applied for 100% quality control of cast parts.

After a brief description of the measurement technique and experimental setup used to carry out the tests, main results and discussion are reported. Most emphasis has been addressed to assess the influence of different operative parameters on defect's detection capability as well as accurate sizing of the discontinuity.

1. Introduction

In the last decades, the industrial interest on the development of advanced non-destructive techniques for the qualification of materials and products has been increased noticeably. As example, the investigation of internal discontinuities such as voids, porosity, shrinkage, slag and inclusions in cast iron turbo parts is today carried out routinely using x-ray and γ-ray radiography [1]. In parallel, ultrasounds represent another characterization technique that has been extensively studied for application as quality control tool in casting production [2-3].

The above mentioned techniques can be considered as well known methods, and devices based on such a technologies are today widely available in commerce. In recent years, researchers are pointing their efforts towards the development of new non-destructive testing (NDT) methods which allow for fast, no contact and reliable manufacturing quality control. Among these, active infrared thermography (AIT) is one of the most promising one. In AIT, thermal waves are used to excite the specimen in order to induce significant temperature differences witnessing the presence of subsurface anomalies [4]. A large variety of sources, which include either optical, electromagnetic or acoustic excitation, have been successfully experimented to generate a thermal path into the part to be inspected. Meanwhile, signal to noise ratio and detection capability have been drastically improved using lock-in thermography [5-8], where the process of bandwidth reduction makes use of the complete coded information contained in the sequence of thermograms recorded at one single modulation frequency.

This paper explores the use of ultrasound excited lock-in thermography (ULT) as an effective method for the inspection of cast iron turbocharger components. Due to its exceptionally fast response, the proposed method could potentially be applied for 100% inspection of complex castings parts, with notably time and economic saving when compared to well established NDT techniques. After a brief description of the measurement principle, the attention is first focused on evaluating the influence of different working parameters (carrier frequency, modulation frequency, ultrasound excitation power, number of heating cycles) on defect's detection capability and on the optimization of the experimental setup (choice of the "best parameters set") for the specific application. Finally, phase thermal images obtained on both defected and sound parts are reported and a fast algorithm for defect's sizing is presented.

2. Ultrasound lock-in thermography

ULT uses ultrasound-generated heat as defect detection mechanism. The basic principle is based on theory that as defects may be areas where mechanical damping and friction losses primarily take place, the vibro-acoustic energy is converted into heat mainly in defects than in sound areas, resulting in a defect selective dark field method [9]. Thus, in contrast to energy deposition by means of external heat sources, ultrasound excited thermography uses internal heat generation by inducing high-frequency elastic waves into the sample. On the other hand, ultrasonic excitation signals may trigger mechanical resonances causing the formation of unwanted standing waves that might appear as a superposed temperature pattern hiding defects [10].

http://dx.doi.org/10.21611/qirt.2010.097
10th International Conference on Quantitative InfraRed Thermography

By modulating the high frequency ultrasound amplitude excitation with a low frequency lock-in signal the signal to noise ratio can be greatly enhanced [11], as in optical lock-in thermography. Hence, the resultant periodical temperature pattern generated at the surface, expressed as a function of depth *z* and time *t*, given by (one-dimensional model, [4]):

$$T(z,t) = T_0\, e^{-z/\mu} \cos\left(\omega t - \frac{2\pi z}{\lambda}\right) \tag{1}$$

can be evaluated through its emission in the MWIR range and reconstructed by means of four equidistant data points S_i (x,y) recorded over the specimen surface during each modulation period [12]. These four images are then processed in the frequency domain using the Fourier transformation tuned to the frequency of amplitude modulation to gain the magnitude image $A(x,y)$ and the phase image $\phi(x,y)$:

$$A(x,y) = \sqrt{\left[S_1(x,y) - S_3(x,y)\right]^2 + \left[S_2(x,y) - S_4(x,y)\right]^2} \tag{2}$$

$$\phi(x,y) = \tan^{-1}\left[\frac{S_1(x,y) - S_3(x,y)}{S_2(x,y) - S_4(x,y)}\right] \tag{3}$$

These two parameters are used to present the relevant information about subsurface discontinuities. Phase angle imaging has many advantages, since artefacts resulting from inhomogeneities of emission coefficient or ultrasound power deposition are reduced significantly. In addition, information about defect depth can be obtained by varying the lock-in frequency, because of the dependence of the phase shift on the propagation time of the thermal wave travelling from the defect site to the surface.

Nonetheless, actually there are also some factors limiting the performance of ULT, which include allowable modulation frequency, ultrasound power limit and noise of the thermographic system (thermal and time resolution).

Ultrasound excited thermography has been proposed in recent years as an effective NDT method in a number of applications, such as imaging of aerospace structures [13-16], non-destructive testing of adhesive joints and riveted structures [17], maintenance of CFRP rims [18] and crack detection for applications in the automotive industry [19-20].

3. Experimental set-up

A batch of several defected and sound cast iron turbo housing samples (figure 1a), with two different geometries (namely type 1 and type 2), were provided by a leading Italian foundry, holding 30% of the world-wide market in castings for turbochargers. Each sample was first examined by x-ray radiography and 3D computed tomography and then subjected to thermographic NDE.

The experimental setup used in our study basically consists of a high resolution infrared camera, a ultrasound generation unit, a pneumatically-driven coupling system and a control unit for software lock-in. The infrared camera (FLIR Titanium 560 M) has a 640 x 512 pixels InSb FPA detector working in the MWIR (3.6 – 5.1 μm) spectral band and was equipped with a 50 mm F2 focal length lens. The NETD was stated by the manufacturer to be better than 20 mK at ambient temperature. A 2.2 kW digital ultrasound generator coupled to a pneumatically controlled resonance unit including a damped piezo-ceramic converter, a booster and a sonotrode were used to optimize ultrasound injection into the sample (figure 1 b).

a)

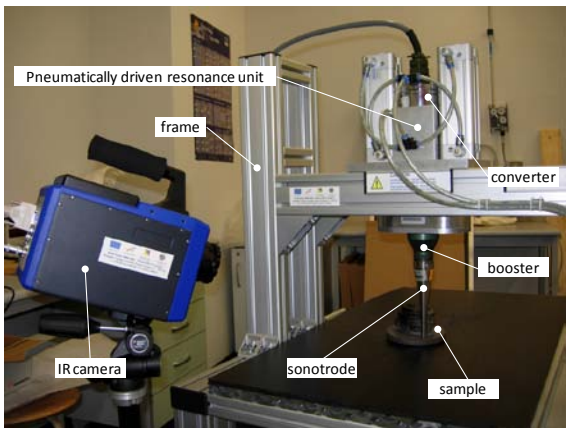

b)

Fig. 1. *a) cast iron turbo housing sample (type 2) and b) experimental set-up for ultrasound excited thermography*

http://dx.doi.org/10.21611/qirt.2010.097

The allowable range for the excitation frequency generated by the ultrasonic converter was approximately 15 kHz – 25 kHz with adjustable amplitude from 0% to 100%. The carrier frequency was modulated using low-frequency sinusoidal signals (lock-in mode) set between 0.01 Hz and 1 Hz. The temperature modulation at the surface was analysed by tuning the IR camera acquisition to the frequency of amplitude modulation. The DisplayIMG ver.2.6 software (Edevis GmbH, Germany) was used to control the acquisition and record thermal images.

Special care was reserved to ensure efficient acoustic coupling and impedance matching between the sonotrode tip and cast sample surface, which is not planar: best results were obtained by interposing a 3 mm thick Teflon strip between the two coupling surfaces.

4. Experimental results

4.1. Definition of the working parameters: sensitivity analysis

Preliminary tests were carried out in order to investigate the influence of different working parameters on the normalized phase contrast, which has been defined as follows:

$$C^n(t_f) = \frac{\Delta\varphi(t_f)}{\varphi_s(t_f)} = \frac{\varphi_{def}(t_f) - \varphi_s(t_f)}{\varphi_s(t_f)} \qquad (4)$$

where $\varphi_{def}(t_f)$ and $\varphi_s(t_f)$ are the average phase values of defected and sound regions, measured at the end time t_f of the thermal process over a small circular area (4 mm diameter) of the thermogram.
The following parameters were considered:

1. excitation frequency f_c (15 kHz ... 25 kHz, with 0.5 kHz step increment)
2. number of heating periods N (1 ... 20)
3. nominal amplitude of ultrasound power $P_{\%}$ (1 ... 30%)
4. frequency of amplitude modulation f_m (0.01 Hz ... 1 Hz)

Sensitivity analyses were then carried out by varying each single parameter keeping the other ones constant.

Figure 2a shows the thermo-acoustic spectrum computed over the defected area by wobbling the excitation frequency from 15 kHz to 25 kHz. The thermo-acoustic spectrum can guide the selection of optimal excitation frequency for lock-in measurements. By observing the graph, three resonance frequencies causing significant temperature increments are observed at 19476 Hz, 20396 Hz and 24996 Hz, respectively. Figure 2b shows the effect of the excitation frequency on the normalized contrast in lock-in mode. These tests were done by fixing all the parameters (f_m=0.05 Hz, N=1, $P_{\%}$=12) while rising the excitation frequency step by step up to 25 kHz. For each frequency, tests were repeated three times. By comparing the two plots of figures 2a and 2b, a good correlation can be highlighted, although not all the resonance peaks observed in the thermo-acoustic spectrum actually lead to an appreciable phase contrast in amplitude modulated measurements. One reason of this behaviour might be attributed to the different duration of the excitation between the two experimental tests: the multy-frequency test, in fact, takes 100 s to sweep the whole frequency range, while lock-in measurements were modulated at 0.05 Hz (test duration 20 s). Hence, the overall heating of the sample was actually higher in the second case, leading to a considerable reduction of either amplitude or phase contrast. In addition, monofrequent excitation can produce superimposed temperature patterns caused by standing elastic waves due to vibrational resonance matching (e.g., 23.5 kHz point data in figure 2b). Both results indicate 25 kHz as the optimal excitation frequency (maximum temperature rise, maximum normalized contrast), hence this value was used to carried out all the following tests.

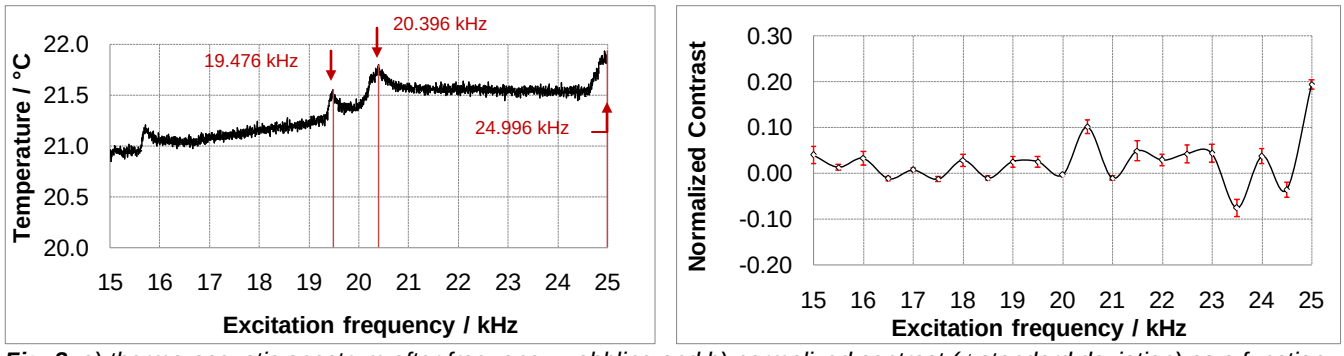

Fig. 2. *a) thermo-acoustic spectrum after frequency wobbling and b) normalized contrast (± standard deviation) as a function of the excitation frequency measured in lock-in mode with 0.05 Hz amplitude modulation (N=1, $P_{\%}$=12)*

http://dx.doi.org/10.21611/qirt.2010.097
10th International Conference on Quantitative InfraRed Thermography

The effect of the number of heating periods on defect detection is reported in figure 3a. These tests were performed with f_m=0.05 Hz, f_c=25 kHz and $P_{\%}$=12. As practical NDT routines based on ULT have to be implemented along a production line, this parameter is important, since it is directly related to the total cycle time of the conformity verification test. By increasing the number of cycles from 1 to 15, the normalized contrast computed over the defect area rises twofold. At the same time, the obtained results provide evidence that the discontinuity can be reliably detected even if a single modulation period is used (cycle time 20 s).

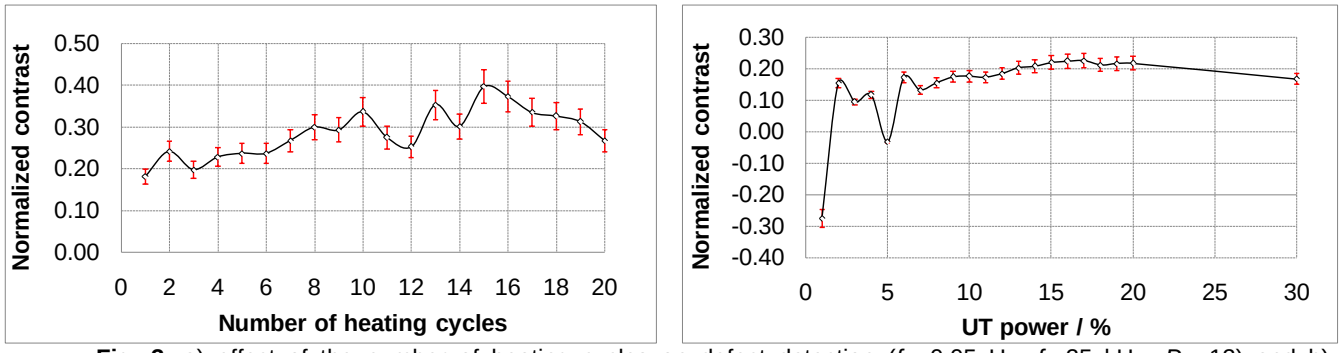

Fig. 3. a) effect of the number of heating cycles on defect detection (f_m=0.05 Hz, f_c=25 kHz, $P_{\%}$=12) and b) normalized contrast as a function of percentage ultrasound power (errors bars showing ± standard deviation on three repeated measurements) (f_m=0.05 Hz, f_c=25 kHz, N=1)

The effect of nominal amplitude of ultrasound power is illustrated in figure 3b. These tests were performed with f_m=0.05 Hz, f_c=25 kHz and N=1.This parameter has little influence on the normalized phase contrast, providing an adequate (> 6%) amplitude intensity is transferred to the part. Hence, as far as applications on casting are concerned, our results suggest that high power excitation is not necessary to identify the discontinuity, thus reducing the risk of local damage due to a significant thermal load during the ultrasonic excitation.

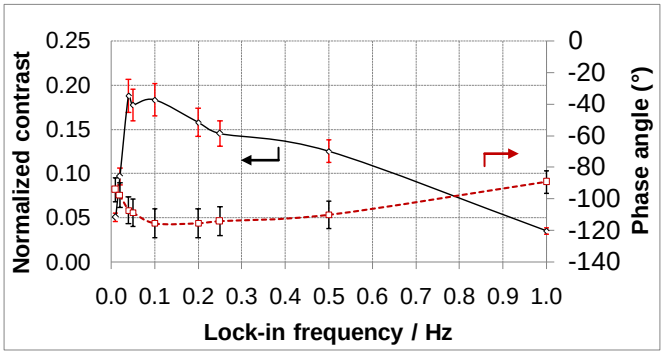

Fig. 4. Effect of the modulation frequency on normalized contrast computed over the defected area and phase angle plot (errors bars showing ± standard deviation on three repeated measurements) (f_c=25 kHz, $P_{\%}$=12, N=1)

The correlation between the lock-in frequency and the normalized contrast is investigated in figure 4. These tests were performed with f_c=25 kHz, $P_{\%}$=12 and N=1. As it can be observed, the phase angle difference reaches a maximum for modulation frequencies between 0.04 Hz and 0.1 Hz. By assuming a one-dimensional model (1) for the thermal wave field [4], the depth range of the defect may be estimated as (being α = 0.15 cm^2/s the material thermal diffusivity, ω= 2πf the angular frequency, μ the thermal diffusion length)

$$z \cong 1.8\mu = 1.8\sqrt{\frac{2\alpha}{\omega}} \qquad (5)$$

which yields a defect depth extension between 12.4 mm and 19.7 mm. These values are roughly 2.5 times larger than the actual ones, leading to the conclusion that the use of a simplified model for thermal wave field prediction is not adequate in this case and more complex numerical models have to be implemented in order to estimate defect depth.

http://dx.doi.org/10.21611/qirt.2010.097

4.2. Defects detection

On the ground of preliminary sensitivity tests reported in the previous section, the following set of optimal parameters was selected: f_c=25 kHz, f_m=0.05 Hz, $P_{\%}$=*12* and N=1.

The following figures highlight the main results obtained by examining several defected and sound samples of two distinct types of cast iron turbocharger housings, having a slightly different geometry and identified as type 1 and type 2, respectively. The samples were furnished as cast and were not subjected to neither further processing nor surface finishing, so that the applicability of the proposed ULT technique along the production line could be assessed.

Figure 5 refers to the type 1 housing geometry. The overall cycle time of a typical test was about 30 s, including positioning of the sample on the test bench. The sample 1a presents a solidification shrinkage void (lack of fusion) subsurface discontinuity in the front view that was easily detected by ultrasound excited lock-in thermography. The unfilled region, located along the circumferential transition between the two cylindrical volumes that form the upper part of the turbo housing, is about 5 mm wide and extends to a depth of 7.8 mm, as empathized by CT slices computed by means of an x-ray tomographic scan (further details are given in the figure's caption). The minimum distance to the measured surface is roughly 2 mm. For comparison purpose, phase thermograms obtained on a sound sample (1b) belonging to the same production batch are also reported in the figure.

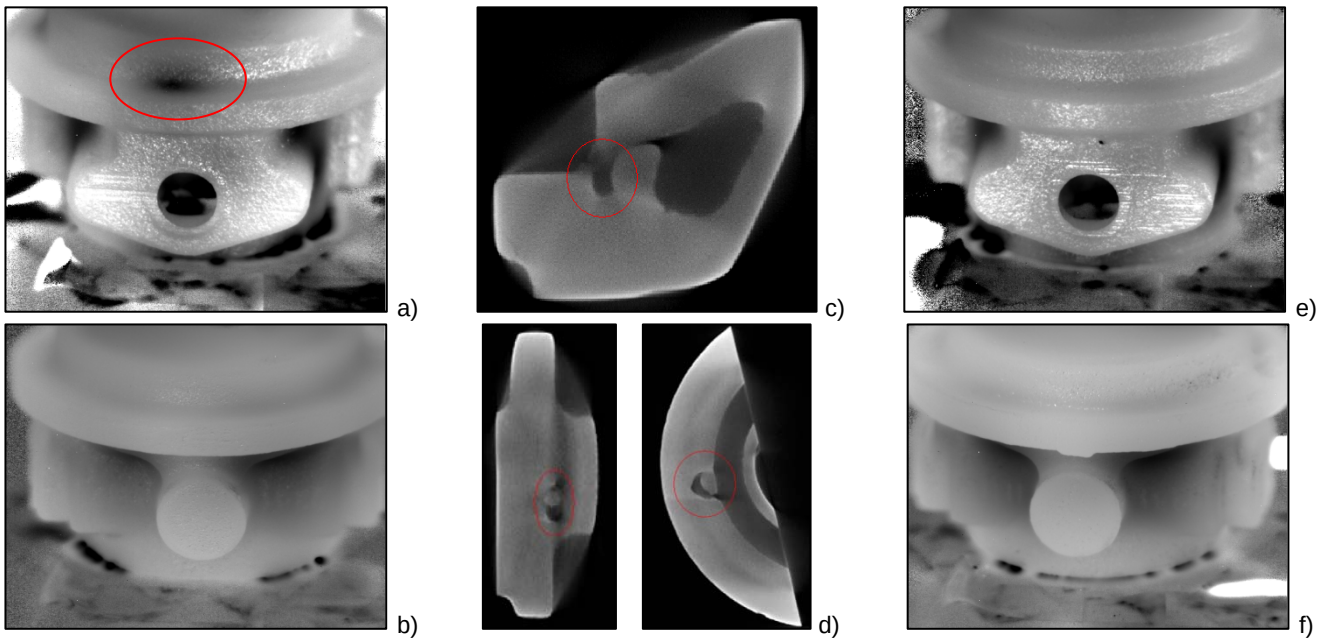

Fig. 5. ULT nondestructive testing results on type 1 cast iron turbo components (coupling: PTFE, modulation frequency: 0.05 Hz, UT excitation frequency: 25 kHz, UT amplitude: 12%, number of preheating/heating cycles:0/1): a) gray level phase image of sample 1a (defected, front view); b) gray level phase image of sample 1a (sound, back view); c-d) CT slices of sample 1a computed by means of variable focus 225 kV x-ray tomography (V_{acc} = 160 kV; A_{acc} = 1.50 mA; focus spot = 800 mm): radial section (top), vertical section (bottom left) and horizontal section (bottom right); e) gray level phase image of sample 1b (sound, front view); f) gray level phase image of sample 1b (sound, back view)

Figure 6 refers to the type 2 housing geometry. Similar sensitivity tests as those reported in the section 4.1 for the type 1 geometry were performed in order to find an optimal set of working parameters (f_c=22 kHz, f_m=0.05-0.2 Hz, $P_{\%}$=*12* and N=1). The overall cycle time was typically around 20 s, including positioning of the sample on the test bench. The sample 2a presents a porosity discontinuity located on the larger diameter region of the turbo housing. The flaw, as confirmed by the γ-ray radiography shown in the same figure, has multi-segmented spots that covers an area of about 11 mm width, at about 3.5 mm from the measured surface. Results are presented for slightly different values of the lock-in frequency to show how this parameter influences defect's detectability. In the same figure, phase thermograms of a sound sample (2b) belonging to the same production batch are shown for comparison.

It has to be noted that, although the results presented in this study clearly proved that ULT was able to identify the presence of defects in a reliable and repeatable way, it does not provide information about the nature of the discontinuity: defects of different origin in cast iron components, such as slag inclusions, cracking, porosity and solidification shrinkage voids, are likely to produce similar thermal signature.

http://dx.doi.org/10.21611/qirt.2010.097
10th International Conference on Quantitative InfraRed Thermography

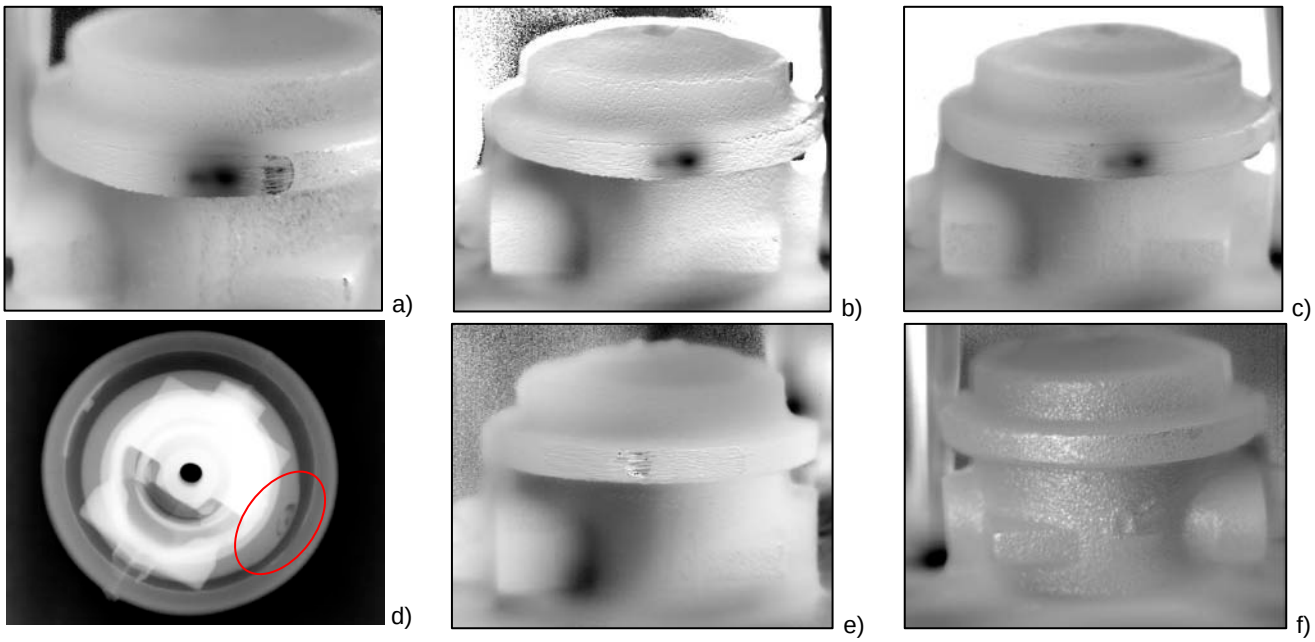

Fig. 6. ULT nondestructive testing results on type 2 cast iron turbo components (coupling: PTFE, UT excitation frequency: 22 kHz, UT amplitude: 12%, number of preheating/heating cycles:0/1): a) gray level phase image of sample 2a obtained with 0.2 Hz modulation (defected, front view); b) gray level phase image of sample 2a obtained with 0.1 Hz modulation (defected, front view); c) gray level phase image of sample 2a obtained with 0.05 Hz modulation (defected, front view); d) γ-ray radiography of sample 1a showing the subsurface multi-segmented macro porosity; e) gray level phase image of sample 2b obtained with 0.05 Hz modulation (sound, front view); f) gray level phase image of sample 2a obtained with 0.05 Hz modulation (sound, back view)

4.3. Defects sizing

A simple yet effective semi-automatic method has been developed to process phase images for defect size assessment (figure 7). The algorithm, built up in the Matlab® environment, works according to a histogram-based image segmentation based on iterative thresholding. Starting from the measured phase image, a region of interest (ROI) is first defined by the user. Then, the gray-level histogram of the windowed image is analysed and the image segmented using a "first tentative" threshold value. Hence the threshold *TH* is varied recursively to some extent and the results weighted using a knowledge matrix to search for an optimal *TH* value.

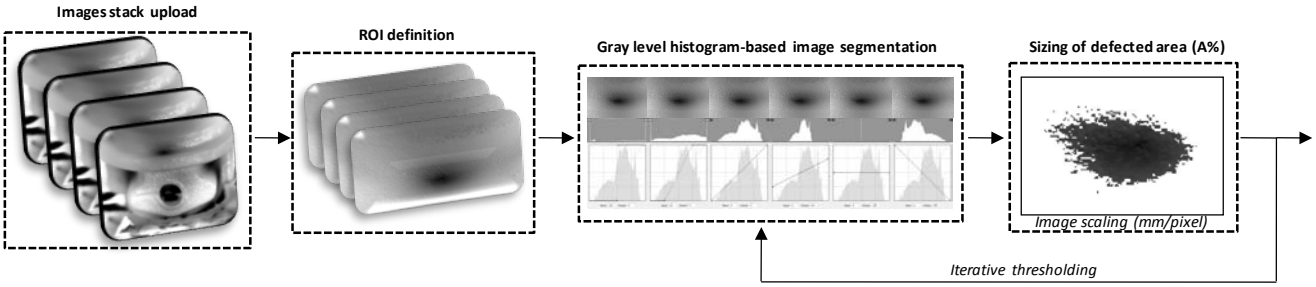

Fig. 7. Flow chart of the algorithm used for defect size assessment

The histogram-based algorithm can also be quickly adapted to process multiple frames. Hence, it can be used to compare several parametrized phase images to find out optimal working parameters for the specific application. As an example, Figure 8 reports the results obtained by processing stacks of phase images recorded by varying the excitation frequency (*meanFexc*), the modulation frequency (*meanFlockin*) and the percentage amplitude of ultrasound power (*meanAmp*). The maximum of each curve identifies the image number corresponding to the "best value" phase image in term of defect detectability. The following values were obtained: f_{amp}=6%, f_m=0.1 Hz, f_c=25 kHz. These values agree well with those reported in section 4.1.

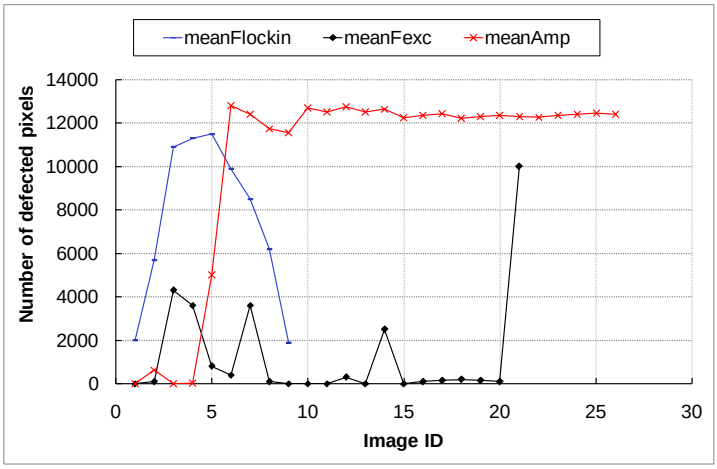

Fig. 8. Plot of parameterized average defected pixels within the ROI. The number displayed on the *x*-axis labels phase images ordered with increasing values of the specific parameter used: excitation frequency (*meanFexc*), modulation frequency (*meanFlockin*) and percentage amplitude of ultrasound power (*meanAmp*).

5. Conclusions

This paper explored the use of ultrasound activated infrared thermography for quality control assessment in castings. The experimental approach is based on selective heating of inner flaws in cast iron turbo housings by means of high frequency ultrasonic waves modulated in amplitude by a lock-in sinusoidal signal. The effectiveness of the proposed measurement technique has been demonstrated throughout several examples showing reliable defect's detection of subsurface discontinuities located up to 3.5 mm depth. The overall cycle time was typically around 30 s, including positioning of the sample on the test bench. A simple and fast algorithm for defect's sizing based on automatic recognition of the gray levels distribution within the phase thermal image was presented. The algorithm can process several images in few seconds, allowing the percentage defected area within the ROI to be estimated almost in real-time and user-defined acceptance/rejection criteria to be easily established. This is an important requisite for the practical implementation of this nondestructive testing technique in 100% quality control industrial protocols. Nevertheless, also drawbacks exist: the proposed technique failed in discriminating between discontinuities of different origin. In addition, more complex models for thermal wave field prediction than the simple one-dimensional one are compulsory for accurate defect's depth estimation.

Acknowledgements

The authors wish to thank Dr. Marcello Montini (technical director) and Dr. Emiliano Mingardi (research assistant) of Fonderie Officine Meccaniche Tacconi (Perugia, Italy) for providing cast iron samples and technical support. The assistance of Mr. Riccardo Bartolucci in the development of the image processing algorithm is also acknowledged.

The work was partially financed under the research project "Centro Ricerche Tecna Territorio – PIT 22" POR SICILIA 2000-06 – Misura III.15 Azione C n. 1999.IT.16.1.PO.011/3.15/5.2.13/0017.

REFERENCES

[1] Bossi R. H., Iddings F. A., Wheeler G. C., Nondestructive Testing Handbook, Third Edition: Volume 4, Radiographic Testing, The American Society for Nondestructive Testing, USA, 700 p., 2002.
[2] Shull P. J., Nondestructive evaluation, theory, techniques and application, Marcel Dekker ed., 841 p., 2002.
[3] Lofaj F., Seldis T., Nilsson K. F., Eriksson A., Ultrasonic Study of Defects in Ductile Cast Iron Inserts For Spent Nuclear Fuel Disposal, 9th European NDT Conference, September, 25-29, Berlin, 2006.
[4] Maldague X., Theory and practice of infrared technology for nondestructive testing, J. Wiley & Sons ed., New York, 684 p., 2001.
[5] Carlomagno G. M. and Berardi P. G., "Unsteady Thermography in Non-Destructive Testing," in Proceedings of the 3rd Biannual Information Exchange, St. Louis/USA, pp. 33–40, 1976.
[6] Busse G., "Optoacoustic phase angle measurement for probing a metal", Appl. Phys. Lett. 35, p. 759–760, 1979.
[7] Lehto A., Jaarinen J., Tiusanen T., Jokinen M., Luukkala M., "Amplitude and phase in thermal wave imaging", Electr. Lett. 17, pp. 364-365, 1981.

[8] Busse G., Wu D., Karpen W., "Thermal wave imaging with phase sensitive modulated thermography," J. Appl. Phys., vol. 71, p. 3962–3965, 1992.
[9] Mignogna R. B., Green R. E., Duke J., Henneke E. G., Reifsnider K. L., "Thermographic investigation of high-power ultrasonic heating in materials", Ultrasonics 7, p.159-163, 1981.
[10] Salerno A., Dillenz A., Wu D., Rantala J., Busse G., "Progress in ultrasound lockin thermography", in Proceedings of Quantitative Infrared Thermography (QIRT 98), Lodz, p.154-160, 1998.
[11] Rantala J., Wu D., Busse G., "Amplitude modulated lock-in vibrothermography for NDE of polymers and composites", Res. Nondestr. Eval. 7, p. 215-218, 1996.
[12] Wu D., Busse G., "Lock-in thermography for non-destructive evaluation of materials", Rev. Gén. Therm., vol. 37, p. 693-703, 1998.
[13] Zweschper Th., Dillenz A., Busse G., "Ultrasound lockin thermography – a defect-selective NDT method for the inspection of aerospace structures", Insight, vol. 43(3), p. 173-9, 2001.
[14] Zweschper Th., Dillenz A., Riegert G., Scherling D., Busse G., "Lockin thermography methods for the NDT of CFRP aircraft components", in Proceedings of 8th European Conference on NDT, Barcelona, Spain, 2002.
[15] Busse G., Dillenz A., Zweschper Th., "Defect-selective imaging of aerospace structures with elastic wave activated thermography", in Proceedings of International Conference on Thermal Sensing and Imaging Diagnostic Applications (Thermosense XXIII), Orlando, Florida, 2001.
[16] Zweschper Th., Dillenz A., Riegert G., Scherling D., Busse G., "Ultrasound excited thermography using frequency modulated elastic waves", Insight, vol. 45 (3), p.178-82, 2003.
[17] Zweschper Th., Dillenz A., Busse G., "NDE of adhesive joints and riveted structures with lock-in thermography methods", in Proceedings of International Conference on Thermal Sensing and Imaging Diagnostic Applications (Thermosense XXIII), Orlando, Florida, 2001.
[18] Gleiter A., Spießberger C., Busse G., "Lock-in thermography with optical or ultrasound excitation", in Proceedings of the 10th International Conference of the Slovenian Society for Non-Destructive Testing, Ljubljana, Slovenia, 2009.
[19] Zweschper Th., Riegert G., Dillenz A., Busse G., "Ultrasound burst phase thermography (UBP) for applications in the automotive industry", in Proceedings of 29th Annual Review of Progress in Quantitative Nondestructive Evaluation, Washington D.C., 2002.
[20] Gleiter A., Spießberger C., Zweschper Th., Busse G., "Improved ultrasound activated lockin-thermography using frequency analysis of material defects", Journal of Quantitative Infrared Thermography, vol. 4(2), p.155-164, 2007.